Available online at www.sciencedirect.com
ScienceDirect
Bioorganic & Medicinal Chemistry 14 (2006) 8396–8404
Bioorganic & Medicinal Chemistry

Discovery of novel, highly potent and selective β-hairpin mimetic CXCR4 inhibitors with excellent anti-HIV activity and pharmacokinetic profiles

Steven J. DeMarco,[a] Heiko Henze,[a] Alexander Lederer,[a] Kerstin Moehle,[a] Reshmi Mukherjee,[a,†] Barbara Romagnoli,[a] John A. Robinson,[a] Federico Brianza,[b] Frank O. Gombert,[b] Sergio Lociuro,[b,‡] Christian Ludin,[b] Jan Willem Vrijbloed,[b] Jürg Zumbrunn,[b] Jean-Pierre Obrecht,[b] Daniel Obrecht,[b,*] Vincent Brondani,[c] François Hamy[c,§] and Thomas Klimkait[c]

[a]*Chemistry Department, University of Zürich, Winterthurerstrasse 190, 8057 Zürich, Switzerland*
[b]*Polyphor AG, CH-4123 Allschwil, Switzerland*
[c]*InPheno AG, CH-4051 Basel, Switzerland*

Received 10 May 2006; revised 26 August 2006; accepted 6 September 2006
Available online 28 September 2006

Abstract—Novel highly potent CXCR4 inhibitors with good pharmacokinetic properties were designed and optimized starting from the naturally occurring β-hairpin peptide polyphemusin II. The design involved incorporating important residues from polyphemusin II into a macrocyclic template-bound β-hairpin mimetic. Using a parallel synthesis approach, the potency and ADME properties of the mimetics were optimized in iterative cycles, resulting in the CXCR4 inhibitors POL2438 and POL3026. The inhibitory potencies of these compounds were confirmed in a series of HIV-1 invasion assays in vitro. POL3026 showed excellent plasma stability, high selectivity for CXCR4, favorable pharmacokinetic properties in the dog, and thus has the potential to become a therapeutic compound for application in the treatment of HIV infections (as an entry inhibitor), cancer (for angiogenesis suppression and inhibition of metastasis), inflammation, and in stem cell transplant therapy.

1. Introduction

The α-chemokine stromal-derived factor (SDF)-1α (also known as CXCL12) binds to the transmembrane G-protein coupled receptor CXCR4. CXCR4 was first discovered as a co-receptor, with CD4, for the entry of T-cell line-tropic (X4) HIV-1 into T-cells.[1–3] Another chemokine receptor, CCR5, also acts as a co-receptor for HIV, but for the cellular entry into macrophages of (M)-tropic HIV-1.[4–7] The CXCR4-SDF-1 interaction is also a master regulator of normal and cancer stem cell trafficking in the human body,[8–11] and so plays a key role in the progression and metastasis of various types of cancer cells to organs that highly express SDF-1.[12–16] Moreover, CXCR4 in combination with granulocyte colony stimulating factor (G-CSF) has been implicated in hematopoietic stem cell mobilization.[17] In view of these important biological functions mediated by CXCR4, inhibitors of the SDF-1α-CXCR4 interaction[18,19] hold great promise as future therapeutics for the treatment of diseases such as AIDS, cancer, inflammation, and arthritis.

There are to date relatively few small-molecule antagonists of CXCR4 known. In this respect, the SDF-1α-CXCR4 interaction appears to resemble more a protein–protein interaction, where the design of small-molecule inhibitors is notoriously difficult, than a typical GPCR where medicinal chemists have traditionally had greater success in finding small drug-like molecules as receptor ligands. One of the first CXCR4 antagonists

Keywords: CXCR4 inhibitor; Peptide; Protein epitope mimetics; Drug design.
* Corresponding author. Tel.: +41 61 4869898; fax: +41 61 4869869; e-mail: daniel.obrecht@polyphor.com
† Present address: Harvard Medical School, Boston, MA 02459, USA.
‡ Present address: Arpida AG, CH-4142 Münchenstein, Switzerland.
§ Present address: Institut of Med. Microbiology, CH-4003 Basel, Switzerland.

0968-0896/$ - see front matter © 2006 Published by Elsevier Ltd.
doi:10.1016/j.bmc.2006.09.003

described was polyphemusin II (Fig. 1), a naturally occurring 18-amino acid peptide isolated from the American horseshoe crab (*Limulus polyphemus*),[20,21] as well as closely related synthetic analogues such as T22 ([Tyr^{5,12},Lys^{7}]-polyphemusin II) (Fig. 1).[22] The group of Tamamura and Fujii investigated the solution structure of T22 by NMR spectroscopy and found that it adopts a β-hairpin conformation stabilized by two disulfide bonds.[23] The same group subsequently synthesized shortened analogues of T22, such as T140, TC14011, and FC131, which showed improved biological activity and stability.[24] Apart from T22 and related derivatives, other known small-molecule CXCR4 inhibitors include AMD3100,[25–27] AMD070,[18,28] and KRH-1636.[29] However, there is an urgent need for the discovery of new potent and selective CXCR4 inhibitors having improved pharmacokinetic and pharmacodynamic properties, and with a safety profile suitable for human clinical use.

The β-hairpin motif, as seen in T22,[24] is one of the most important and abundant supersecondary structure motifs found at protein interfaces. β-Hairpins are found in surface-exposed loops of many protein families and frequently contain key residues important for protein–protein interactions. Recently, β-hairpin protein epitope mimetics (PEM) in the form of template-bound macrocyclic peptides have been described (Fig. 2) that can adopt stable hairpin structures and inhibit protein–protein interactions.[30] In this context, a convenient template comprises the dipeptide D-Pro-L-Pro, which adopts a relatively rigid type-II′ β-turn, and so can effectively

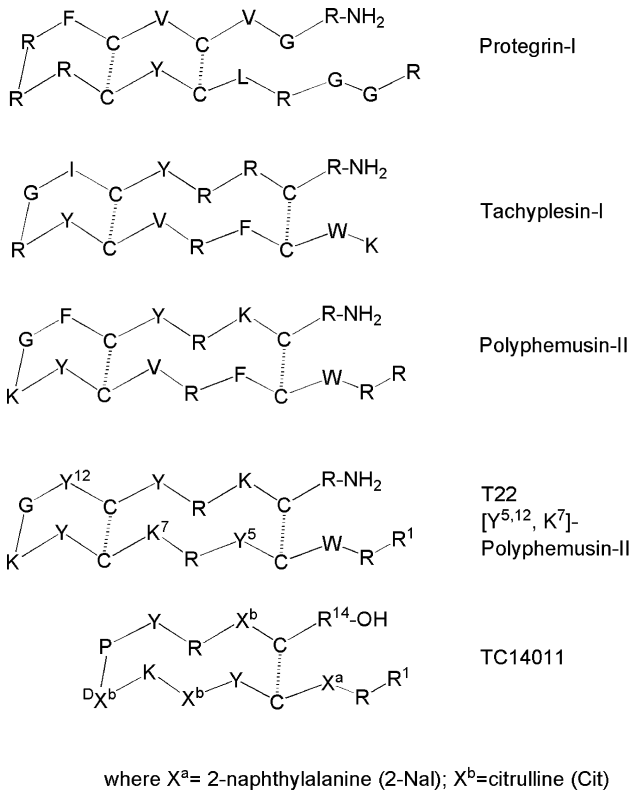

Figure 1. Structures of protegrin-I, tachyplesin-I, polyphemusin-II, T22, and TC14011.

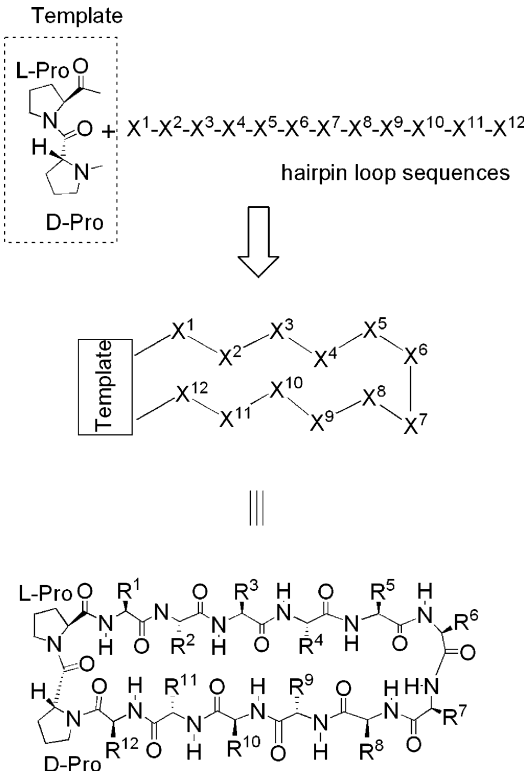

Figure 2. In PEM design, the hairpin sequence of interest (in the case illustrated, 12 residues) is appended to a template (as illustrated, D-Pro-L-Pro) to form a backbone macrocyclic peptide. The template should influence the backbone conformation and help stabilize β-hairpin conformations.

stabilize β-hairpin conformations. Moreover, this template can be incorporated into cyclic PEM molecule conveniently using solid-phase peptide chemistry. The approach to β-hairpin PEM design[30–36] then consists of transplanting a loop sequence from the protein or peptide of interest onto the synthetic template[37,38] (Fig. 2). Additional stabilization of β-hairpin conformations may come by introducing disulfide bonds between cysteine residues located at opposite, non-hydrogen-bonded sites of each β-hairpin strand. Such β-hairpin PEM molecules are readily available by parallel combinatorial synthesis,[30,39] and in several cases stable β-hairpin conformations have been confirmed by NMR-spectroscopy in aqueous solution.[30,39] The cyclic, conformationally constrained backbone of PEM molecules provides a scaffold onto which side-chain groups can be appended to favor binding to a target receptor, and parallel library synthesis and screening provides a powerful handle to optimize both receptor affinity and other pharmacologically relevant ADME properties. Examples of the successful application of this PEM-technology so far include the discovery of mimetics of protegrin I[35] showing good antimicrobial activity, potent inhibitors of serine proteases,[32] as well as inhibitors of the Tat-TAR[29] and p53-HDM2 interactions.[28]

β-Hairpin PEM molecules based on natural products like polyphemusin II, and related antimicrobial peptides such as protegrin I,[36] tachyplesin[40] (Fig. 1), and RTD-1,[41] represent an ideal starting point for the design of

novel antibacterial and antiviral agents. Using this approach to PEM molecule design, we describe here the discovery of novel, potent and selective CXCR4 inhibitors, based on the natural product polyphemusin II.

2. Results

2.1. Design of mimetics

The design of template-bound macrocyclic mimetics started from the truncated polyphemusin-II analogue TC14011, previously reported by Fujii and Tamamura[22,41] (Fig. 1). In a first step, the two residues ᴰCit-Pro at the turn position in TC14011 were replaced by a ᴰPro-ᴸPro dipeptide template, to give POL1638 (Fig. 3). In the next step, a macrocyclic structure was generated by linking the N- and C-terminal residues. This was expected to constrain the conformation, in particular, of the termini and so also to improve resistance to proteolysis. This was achieved by inserting two additional amino acids into the sequence, thereby giving a loop of 14 residues attached to the ᴰPro-ᴸPro template, as shown in Figure 3. Libraries of such macrocyclic peptidomimetics were synthesized, having various combinations of amino acids in the linker region, and their biological properties were assayed (see below). After several iterative rounds of optimization, the mimetics POL2438 and POL3026 were obtained, which showed significantly improved activities in a Ca^{2+}-flux assay (Table 1), and were considerably more stable in plasma and in the presence of liver microsomes (Table 2).

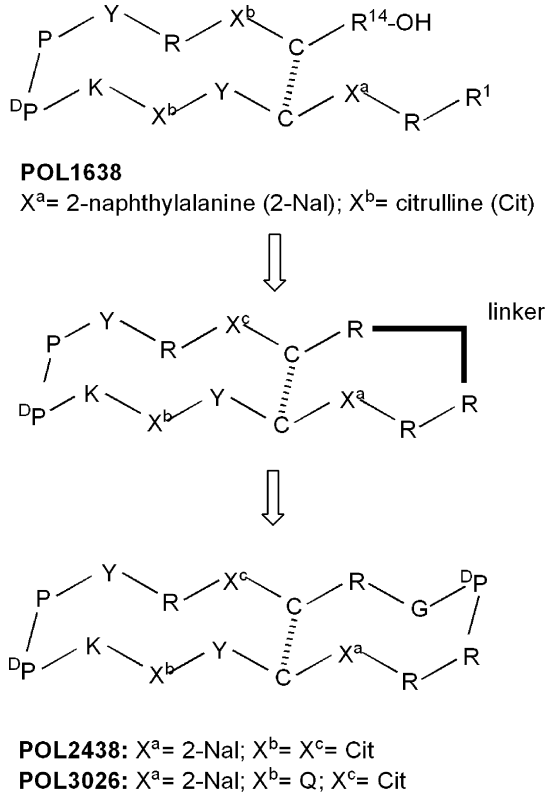

Figure 3. Design of POL2438 and POL3026. See text for discussion.

Table 1. Activity of the PEMs at the CXCR4 receptor

Compound	IC_{50} (nM)	
	Ca^{2+} flux	SDF-1α displacement
TC14011	17.3	nd
POL1638	15.5	100
POL2438	1.9	2
POL3026	1.2	1.2

IC_{50} determination in the Ca^{2+} flux assay and the SDF-1α displacement assay.

2.2. Synthesis of mimetics

The synthesis of POL1638 was performed using Fmoc solid-phase peptide synthesis on highly acid labile chlorotrityl chloride resin. The disulfide bond was installed on the resin, and the product was released by treatment with TFA and purified by reverse-phase HPLC. The synthesis of POL2438 and POL3026 and related analogues was performed in a parallel format also using 2-chlorotrityl resin, as shown in Scheme 1. The disulfide bond was again introduced on-resin, but the macrocyclization was performed in solution. This proceeded efficiently to afford the products typically in 50–80% yields after purification by reverse-phase HPLC. The mimetics were characterized by MS and high resolution ^{1}H NMR. The ^{1}H NMR spectra were fully assigned by standard 2D methods. Although it is beyond the scope of this article to describe fully the conformational properties of all three mimetics, NOESY plots revealed networks of cross-strand NOE connectivities, which show that β-hairpin conformations are significantly populated by all three molecules. Full details of the NMR and MD analyses will be reported elsewhere.

2.3. Biological assays

All compounds were analyzed in a Ca^{2+} flux assay using CXCR4 over-expressing cells, in an SDF-1α (CXCL12) displacement assay (Table 1), as well as for inhibition of chemotaxis (Fig. 4). In addition, in vitro ADME properties, particularly plasma stability, protein binding, and metabolic stability (Table 2), were measured. Inhibition of Ca^{2+} flux, stability in human and rat plasma, and metabolic stability were the main criteria used in optimizing the mimetics.

As shown in Table 1, POL1638 compared well with TC14011 in the Ca^{2+} flux assay. However, not unexpectedly, both compounds showed a limited half-life of 15 and 12 min, respectively, in human plasma. On progressing from the monocyclic disulfide bridged POL1638 to the bicyclic, conformationally constrained POL2438 and POL3026, a factor of 10 in potency was gained (Table 1) as well as a significant improvement in plasma stability (Table 2).

The activity of POL2438 in an assay measuring inhibition of SDF-1α-induced chemotaxis was also performed. Shown in Figure 4 is the inhibition of CEM-SS cell migration as a function of increasing concentrations of POL2438. Using these data, an IMC_{50} value could be

Table 2. In vitro ADME properties of TC14011, POL1638, POL2438, and POL3026

Assay		TC14011	POL1638	POL2438	POL3026
Protein binding	Human (% bound)	71	72	83	54
	Rat (% bound)	nd	nd	76	44
Plasma stability	Human $t_{1/2}$ (min)	12	15	223	>300
	% remaining at 240 min (human)	0	0	51	88
	Rat $t_{1/2}$ (min)	9	15	220	>300
	% remaining at 240 min (rat)	0	0	59	75
Liver metabolization	Human $t_{1/2}$ (min)	nd	nd	>60	53
	Human % metabolized at 60 min	nd	nd	40	59
	Rat $t_{1/2}$ (min)	nd	nd	>60	55
	Rat % metabolized at 60 min	nd	nd	0	31

nd, not determined.

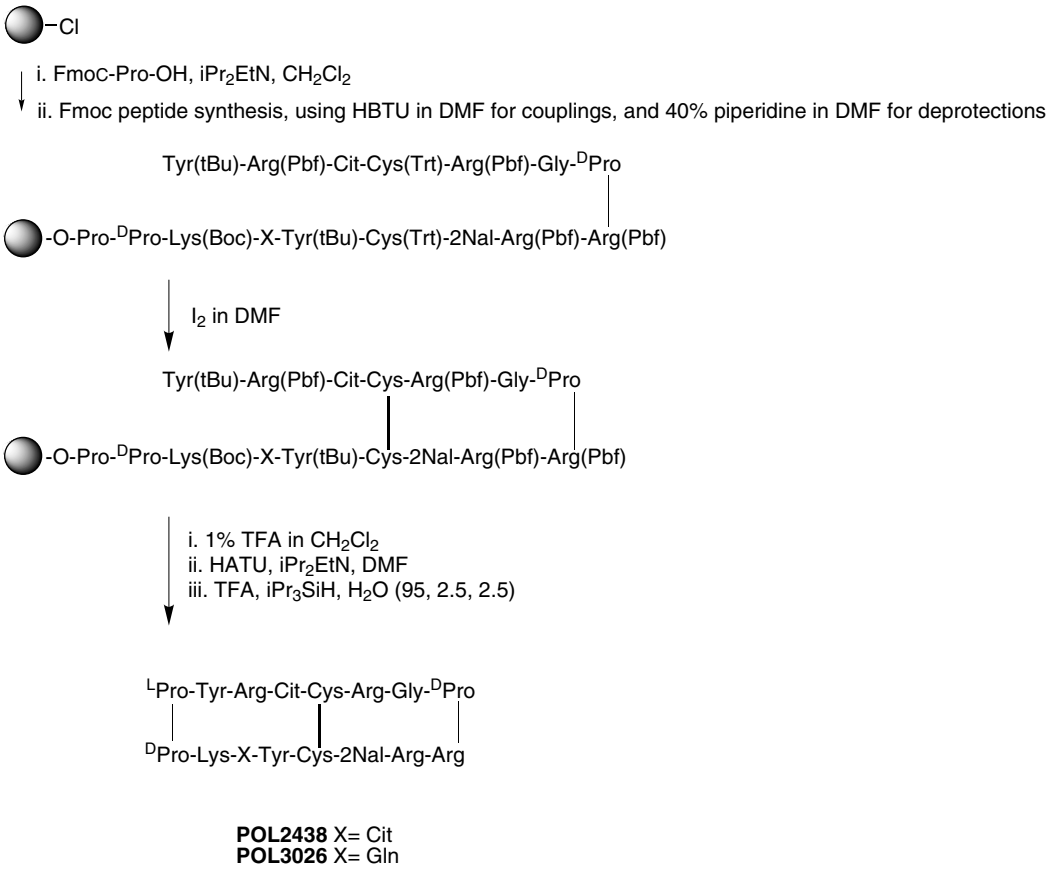

Scheme 1. Synthesis of POL2438 and POL3026.

calculated corresponding to the concentration of POL2438 that inhibits cell migration by 50% in a 1 h period at 37 °C after induction by 1 ng/ml SDF-1α. The IMC_{50} value obtained for POL2438 was 1.2 nM, whereas a selective CCR5 inhibitor showed no inhibition of SDF-1α-driven chemotaxis under the same conditions (data not shown).

In view of the excellent plasma and metabolic stability, POL3026 was selected for further biological studies and for pharmacokinetic (PK) profiling in three male beagle dogs (Fig. 5). After subcutaneous administration of POL3026 at a dose level of 1.5 mg/kg body weight, the mean C_{max} values (1201 ng/ml) were reached 1 h after dosing (T_{max}). After 1 h, plasma levels decreased with an elimination half-life of 3.4 h. The AUC(0–∞) amounted to 4941 ng/h/ml. POL2438 and POL3026 showed excellent selectivity for CXCR4 and showed no significant inhibition of any of the other chemokine receptors tested, including CCR5 (see Section 4).

The high selectivity for CXCR4 versus CCR5 was also confirmed in the deCIPhR assay format, where POL2438 potently inhibited only the T-tropic R4 viruses derived from clinical isolates and not the M-tropic R5 viruses (Fig. 6 and Table 3). The inhibition curves for T-20 (also known as Fuzeon or Enfuvirtide) (Fig. 6b) confirm that recombinant viruses carrying Env-gene taken from patients' viruses present quite a broad range of susceptibility to T20; IC_{50} values reported in Table 3

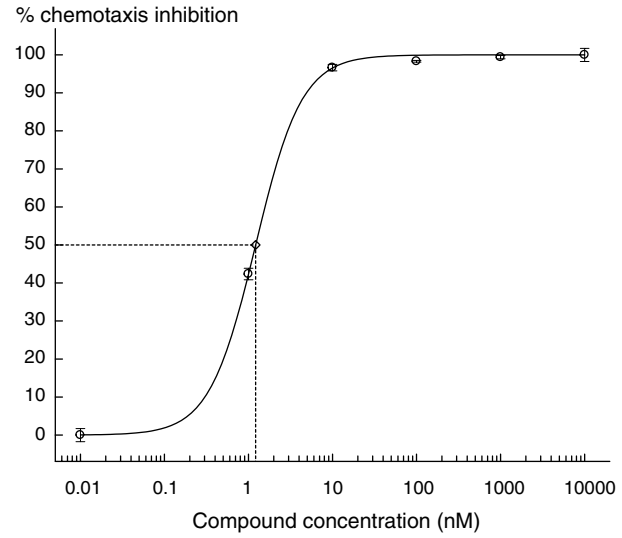

Figure 4. Inhibition of SDF1-α-induced chemotaxis by POL2438.

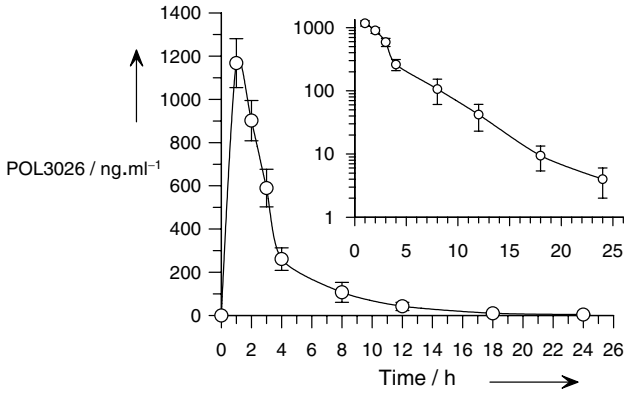

Figure 5. Bioavailability of POL3026. The serum concentration of POL3026 (average of three male beagle dogs) versus time following subcutaneous (open circle) bolus injection. The inset shows the logarithmic concentration-versus-time curve.

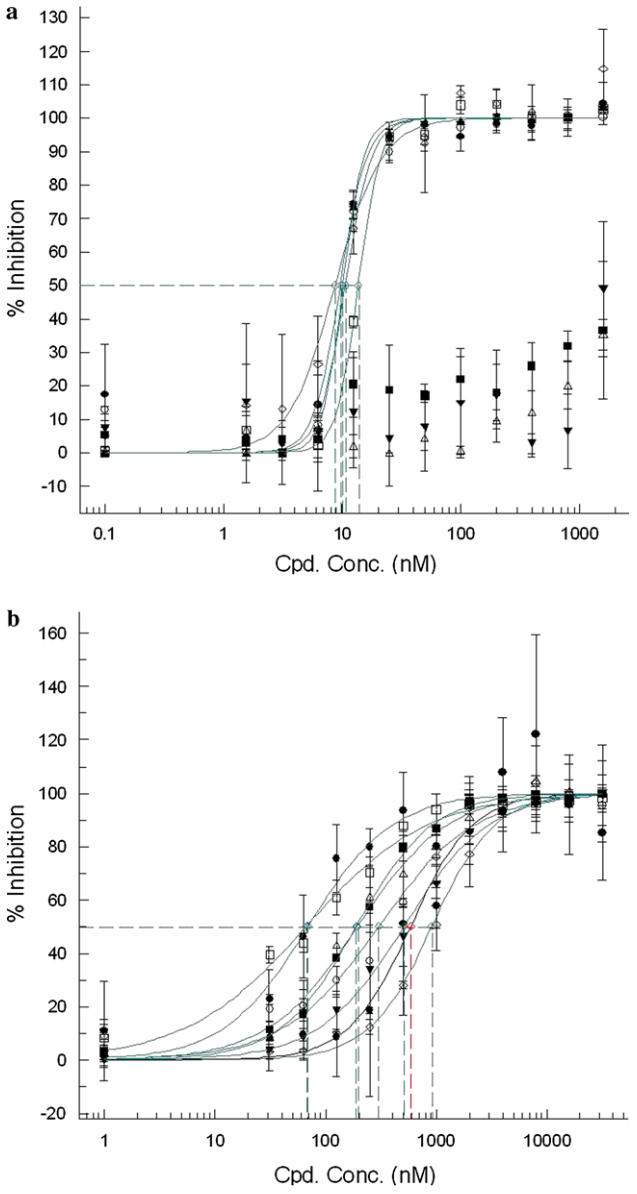

Figure 6. Inhibition of virus entry by POL2438. Viral inhibition curves are shown for 8 recombinant viruses. The IC_{50} values and the co-receptor usage (QXR) determined for each of the 8 virus types are reported in Table 3, along with a key to the symbols used in this figure. (a) Inhibition by POL2438; (b) inhibition by T20.

are across a range of nearly 20-fold. In sharp contrast, inhibition curves for POL2438 (Fig. 6a) distinguish two populations of viruses: a 'sensitive' population, for which the IC_{50} value is tightly grouped near 10 nM, and a 'non-sensitive' population, for which POL2438 shows only minimal activity up to a concentration of 1600 nM. The env genes of the tested viruses were further analyzed, and a prediction of the respective co-receptor tropism was made by employing the heteroduplex tracking assay.[42] The assay revealed that all 'non-sensitive' envelopes in clinical samples belonged to viruses utilizing CCR5 as co-receptor (QXR value >0.76–0.95) (Table 3).

3. Discussion

Inspired by the β-hairpin conformation adopted by the natural product polyphemusin II and the closely related analogues T22, T140, and TC14011[24] (Fig. 1), the design of macrocyclic template-bound β-hairpin mimetics was undertaken to discover novel potent, selective, and metabolically stable inhibitors of CXCR4 having small molecule drug-like ADME properties. POL1638, a close analogue of TC14011, served as a logical structural link to polyphemusin II and a useful starting point for PEM library design. In iterative cycles, PEM libraries were designed, synthesized, and tested, with the aim of improving CXCR4 inhibitory activity as well as metabolic and plasma stability. After synthesis and testing of several hundred analogues, POL2438 and POL3026 were found to be highly potent and stable inhibitors of CXCR4 and were selected for further profiling. It is noteworthy that POL3026 binds at least a thousand fold better to CXCR4 than does AMD3100,[43] a current CXCR4-antagonist in clinical development for stem cell

Table 3. Viral inhibition assays for 8 recombinant viruses; IC_{50} values and co-receptor usage (QXR) are shown

Strain/isolate	Symbol	IC_{50} T20 (nM)	IC_{50} POL2438 (nM)	QXR (R5/X4)
pNL4-3	○	915.8	10.7	<0.05
Env-B	●	66.9	9.7	<0.05
Env-14	◇	69.8	8.7	<0.05
Env-15	△	510.2	>1600	>0.95
Env-11	■	195.3	>1600	0.76
Env-6	□	303.3	13.7	<0.05
Env-C	▲	190.4	10.2	<0.05
Env-17	▼	586.0	>1600	>0.95

The symbols refer to those used in Figure 6. The isolates showing high IC_{50} values (Env-15, Env-11, and Env-17) correspond to R5 specific virus types and so should not be inhibited by POL2438 (as observed).

mobilization. POL3026 constitutes to our knowledge the most active CXCR4 inhibitor described to date.

The high activity of POL3026 and POL2438 was further confirmed in several anti-HIV tests, including in vitro cell fusion assays (FIGS), virus replication assays (deCIPhR), and acute CEM cell infection assays. A comparison was also made to the cell fusion activity of the well-known HIV entry inhibitor T20, which is now marketed under the tradename of Enfuvirtide. It should be noted, however, that T20 is not a chemokine receptor antagonist, but rather blocks a different stage in cellular invasion by HIV. Whereas viruses from a clinical context varied significantly in their response to T20, POL2438 inhibited with high potency all viruses tested utilizing CXCR4 as a co-receptor. Indeed, during the assays, the only viruses in these clinical isolates that showed resistance to the actions of the mimetic were subsequently shown to be M-tropic R5 viruses. These results highlight the high specificity of POL2438 for entry inhibition of T-tropic R4 viruses versus M-tropic R5 viruses. This result may be of clinical relevance as X4 viruses, which replicate best in T-cell lines, often predominate in later stages of HIV infection and may be associated with rapid progression to AIDS and death.[44] In contrast, HIV-1 isolates of the R5 type have been implicated in most cases of sexually transmitted HIV infection. Several selective CCR5 antagonists[19,45] have reached the clinical stage for use in co-receptor HIV entry inhibition. As clinical isolates may contain mixtures of R4 and R5 viruses, or dual-tropic R5R4 viruses, and R5 viruses can switch to R4 viruses, especially at a late stage of disease progression, there is a concern that CCR5 inhibitors may exert a selection pressure favoring X4 viruses. Therefore, it is currently believed that efficient HIV therapy utilizing a co-receptor blockage strategy will require the dual actions of a CCR5 and a CXCR4 antagonist.

Most important, it was possible to significantly improve the initially rather poor in vitro stability and ADME properties of TC14011 and POL1638. The group of Tamamura and Fujii improved the bio-stability of TC14011 through N- and C-terminal modifications such as acetylation or 4F-benzoylation.[46,47] POL3026 showed excellent stability to proteolytic degradation in human plasma, a good plasma protein binding profile, as well as excellent bioavailability following subcutaneous injection in an in vivo PK experiment in dogs. POL3026 thus has the potential to become a novel CXCR4 inhibitor candidate for development as an anti-HIV agent, as an inhibitor of angiogenesis and metastasis, as an agent for the mobilization of hematopoietic stem cells, and to treat inflammation.

4. Experimental

4.1. Peptide synthesis

Peptide synthesis was carried out employing the standard fluorenylmethoxycarbonyl (Fmoc) strategy and the following side-chain protecting groups: Pbf for Arginine, tBu for tyrosine, trityl for cysteine, glutamine and tBoc for lysine. After manual loading of the first amino acid (Fmoc-Arginine(Pbf)-OH for POL1638, and Fmoc-Proline-OH for POL2438 and POL-3026) onto 2-chlorotrityl chloride resin, the linear peptide assembly was performed on a MultiSynTec SyroII peptide synthesizer, typically in a 96-reactor parallel format. At each cycle, 40% piperidine in DMF was employed for Fmoc deprotection followed by coupling of the corresponding amino acid (5 equiv.) using HBTU (5 equiv.) and $^{i}Pr_2EtN$/NMP in DMF. After removal of the final Fmoc group, the resin was swollen in DMF and disulfide bridge formation was carried out using iodine in DMF on the resin. For POL1638, cleavage from the resin and full deprotection was performed using TFA/triisopropylsilane/H_2O (95:2.5:2.5).

For POL-2438 and POL-3026 the disulfide bridged peptides were first cleaved from the resin (1% TFA in CH_2Cl_2) and then cyclized using HATU and $^{i}Pr_2EtN$ in DMF. The fully deprotected peptides were finally obtained employing the same deprotection procedure as described for POL1638.

All the peptides were purified by preparative reverse-phase HPLC (Vydac, 218MS103015, 10 μ C18, 300 Å and Phenomenex, Jupiter, 10 μ C18, 300 Å) and were recovered by lyophilisation. The purity was assessed by analytical reverse-phase HPLC (Vydac, 218MS5215, 5 μ C18, 300 Å; solvent A (H_2O + 0.02% TFA) and B (CH_3CN) and gradient: 0 min: 92% A, 8% B; 8 min: 62% A 38% B; 9–12 min: 0% A, 100% B) and was >95%.

POL1638, retention time 4.35 min, MS, *m/z* 1004.2 [M+H]/2; POL2438, retention time 4.68 min, MS *m/z*

1071.7 [M+H]/2; POL3026, retention time 4.45 min, MS *m/z* 1057.4 [M+H]/2.

4.2. Ca^{2+}-flux assays

CXCR4 transfected 300-19 murine pre-B cells were used according to 48. 300-19-CXCR4 cells were labeled as a batch with Calcium3 Reagent (Molecular Devices, Sunnyvale, CA) in HBSS buffer for 60 min. After dispensing 2.5×10^5 cells in each well of black 96-well plates, a concentrated solution of compound in HBSS + 0.1% BSA was added to the cells. The entire plate was centrifuged and placed in a Flexstation II (Molecular Devices) automated plate reader. After reading a 20 s baseline, the Flexstation dispensed SDF-1α (Peprotech) at a final concentration of 10 nM in HBSS + 0.1% BSA onto the cells and calcium flux was measured for an additional 70 s. The maximum signal was determined from control wells without inhibitor. Percentage of inhibition was calculated from a range of compound concentrations, which were subsequently used to calculate IC_{50} values (Softmax Pro, Molecular Devices). All steps were carried out at room temperature.

4.3. Inhibition of SDF-1α-induced chemotaxis

A Boyden chamber-assay format was used to assess the activity of POL2438 in inhibiting SDF-1α-induced chemotaxis. As starting conditions, a concentration of 1 ng/mL SDF-1α in the lower chamber was selected as chemoattractant for the lymphocytic cells CEM-SS, plated in the upper chamber. After a 1-h incubation, cell migration into the lower chamber was assessed using a colorimetric cell viability assay. Data normalization was performed using the readout of any cells that had migrated in the absence of POL2438. This value was taken as 100% (no inhibitory activity). The graph shown in Figure 4 displays the inhibition of CEM-SS cell migration as a function of increasing concentrations of POL2438 added to the upper chamber at time zero. Using a curve fitting algorithm, which takes into account the standard deviations within the data series, a IMC_{50} value could be calculated as the concentration of POL2438 inhibiting the migration of CEM cells by 50% in a one hour period at 37 °C after induction by 1 ng/mL SDF-1α. As control, a selective CCR5 inhibitor showed no inhibition of SDF-1α-driven chemotaxis under the same conditions (data not shown).

4.4. SDF-1α-AlexaFluor(R)647 displacement assay

CXCR4 competition binding studies with POL1638, POL2438, and POL3026 were carried out using the Fluorokine SDF1-α kit (R&D Systems). Labeled chemokine was incubated with CEM cells and then displaced by increasing concentrations of unlabeled chemokine or inhibitor. Fluorescence was measured by flow cytometry. Maximum (label alone) and minimum (cell autofluorescence) mean histogram fluorescence was adjusted to 100% and 0%. The binding obtained with SDF-1α was 3 nM.

4.5. In vitro ADME assays

4.5.1. Plasma stability. Human plasma (3–5 donors, blood bank SRK, Zürich) and Wistar rat plasma (mixed gender pool >50 animals, Harlan Sera Labs, UK) were used citrate stabilized. The assay was performed in triplicate at 10 μM compound concentration and 37 °C. Samples were taken at 0, 15, 30, 60, 120, and 240 min and stopped by precipitation with 2 volumes of acetonitrile. The supernatant was collected, evaporated, and reconstituted in a 5% acetonitrile solution for analysis by HPLC/MS/MS. The resulting peak area counts were expressed in percent of the zero value and used to determine the endpoint stability in percent, and the half-life. In order to monitor assay integrity, the degradation of propantheline was assayed with every experimental set.

4.5.2. Protein binding. Purified human and rat serum albumins were purchased from Sigma. Compounds were assayed in triplicate for each compound at a 10 μM concentration (albumins at 36 mg/ml end concentration) after an incubation for 1 h at 37 °C. In order to separate bound from unbound compound, samples were filtered on a 96-well 10 kDa filter unit (Millipore) by centrifugation. Filtrates were analyzed by HPLC/MS/MS and the corresponding peak area counts expressed in percent of controls that were similarly incubated and either filtered or not. Propranolol as a reference was assayed with every experimental set.

4.5.3. Metabolic stability. Microsomes from a human 50 donor mixed gender pool and from Sprague–Dawley rat single-gender pools were purchased from InVitro Technologies (Baltimore). The enzymatic reaction was performed in a buffer containing an NADPH regeneration system and microsomes at the following final concentrations: 100 mM potassium phosphate buffer, 1 mg/ml glucose-6-phosphate, 1 mg/ml β-nicotinamide adenine dinucleotide phosphate (NADP), 0.65 mg/ml magnesium chloride, 0.8 U/ml of glucose-6-phosphate dehydrogenase (prediluted with 5 mM citrate buffer), 10 μM compound, and 1 mg/ml microsomal protein (all from Sigma). Compounds were incubated at 37 °C in duplicate and samples taken after 0, 20, and 60 min. After acetonitrile precipitation (2 volumes) and HPLC/MS/MS analysis, metabolic turnover was expressed in % of the initial 0 min value, and half-life was calculated.

4.6. Selectivity of POL1638, POL2438, and POL3026 toward other chemokine receptors

The compounds POL1638, POL2438, and POL3026 were tested for antagonistic activity against a wide variety of chemokine receptors using the calcium flux protocol described above. The following receptor/ligand combinations were used: CCR1/rantes, CCR2/mCP-1, CCR3/Eotaxin, CCR4/MDC, CCR5/rantes, CCR6/larc, CXCR1/Il-8, CXCR2/GROα, CXCR3/IP10, CXCR5/BCA-1, and CXCR6/CXCL16. No significant inhibitory activity was observed against any of the above receptors up to a concentration of 10 μM of peptide.

4.7. Pharmacokinetic profile of POL3026

The pharmacokinetic studies were performed in beagle dogs ($n = 3$) after single subcutaneous administration of 1.5 mg/kg. The $t_{1/2}$ is roughly 3.5 h and the effective plasma concentration stays above the IC_{50} during 24 h (see Fig. 5).

4.8. Anti-HIV activity of POL2438 on HIV clinical variants

The replicative format of the cellular deCIPhR assay has proven suitable for the assessment of replicating recombinant virus carrying genes from clinical HIV-1 isolates from patients naïve for treatment with any fusion inhibitor.[49] In the frame of this study, a portion of the envelope gene (from V2 in gp120 to the end of gp41) of 7 different clinical isolates was cloned into a pNL4-3 proviral vector, in which the corresponding region had been deleted. The resulting viruses were tested in the deCIPhR system for inhibition by T-20 or by POL2438.

References and notes

1. Chabot, D. J.; Broder, C. C. *J. Biol. Chem.* **2000**, *275*, 23774.
2. Feng, Y.; Broder, C. C.; Kennedy, P. E.; Berger, E. A. *Science* **1996**, *272*, 872.
3. Moore, J. P.; Stevenson, M. *Nat. Rev. Mol. Cell. Biol.* **2000**, *1*, 40.
4. Alkhatib, G.; Combadiere, C.; Broder, C. C.; Feng, Y.; Kennedy, P. E.; Murphy, P. M.; Berger, E. A. *Science* **1996**, *272*, 1955.
5. Dragic, T.; Litwin, V.; Allaway, G. P.; Martin, S. R.; Huang, Y.; Nagashima, K. A.; Cayanan, C.; Maddon, P. J.; Koup, R. A.; Moore, J. P., et al. *Nature* **1996**, *381*, 667.
6. Veazey, R. S.; Klasse, P. J.; Schader, S. M.; Hu, Q.; Ketas, T. J.; Lu, M.; Marx, P. A.; Dufour, J.; Colonno, R. J.; Shattock, R. J., et al. *Nature* **2005**, *438*, 99.
7. Kazmierski, W.; Bifulco, N.; Yang, H.; Boone, L.; DeAnda, F.; Watson, C.; Kenakin, T. *Bioorg. Med. Chem.* **2003**, *11*, 2663.
8. Bleul, C. C.; Farzan, M.; Choe, H.; Parolin, C.; Clark-Lewis, I.; Sodroski, J.; Springer, T. A. *Nature* **1996**, *382*, 829.
9. Nagasawa, T.; Kikutani, H.; Kishimoto, T. *Proc. Natl. Acad. Sci. U.S.A.* **1994**, *91*, 2305.
10. Oberlin, E.; Amara, A.; Bachelerie, F.; Bessia, C.; Virelizier, J. L.; renzana-Seisdedos, F.; Schwartz, O.; Heard, J. M.; Clark-Lewis, I.; Legler, D. F., et al. *Nature* **1996**, *382*, 833.
11. Tashiro, K.; Tada, H.; Heilker, R.; Shirozu, M.; Nakano, T.; Honjo, T. *Science* **1993**, *261*, 600.
12. Gerard, C.; Rollins, B. J. *Nat. Immunol.* **2001**, *2*, 108.
13. Muller, A.; Homey, B.; Soto, H.; Ge, N.; Catron, D.; Buchanan, M. E.; McClanahan, T.; Murphy, E.; Yuan, W.; Wagner, S. N., et al. *Nature* **2001**, *410*, 50.
14. Rubin, J. B.; Kung, A. L.; Klein, R. S.; Chan, J. A.; Sun, Y.; Schmidt, K.; Kieran, M. W.; Luster, A. D.; Segal, R. A. *Proc. Natl. Acad. Sci. U.S.A.* **2003**, *100*, 13513.
15. Staller, P.; Sulitkova, J.; Lisztwan, J.; Moch, H.; Oakeley, E. J.; Krek, W. *Nature* **2003**, *425*, 307.
16. Tamamura, H.; Hori, A.; Kanzaki, N.; Hiramatsu, K.; Mizumoto, M.; Nakashima, H.; Yamamoto, N.; Otaka, A.; Fujii, N. *FEBS Lett.* **2003**, *550*, 79.
17. Hendrix, C. W.; Flexner, C.; MacFarland, R. T.; Giandomenico, C.; Fuchs, E. J.; Redpath, E.; Bridger, G.; Henson, G. W. *Antimicrob. Agents Chemother.* **2000**, *44*, 1667.
18. De Clercq, E. *Int. J. Biochem. Cell. Biol.* **2004**, *36*, 1800.
19. Fujii, N.; Nakashima, H.; Tamamura, H. *Expert. Opin. Investig. Drugs* **2003**, *12*, 185.
20. Masuda, M.; Nakashima, H.; Ueda, T.; Naba, H.; Ikoma, R.; Otaka, A.; Terakawa, Y.; Tamamura, H.; Ibuka, T.; Murakami, T., et al. *Biochem. Biophys. Res. Commun.* **1992**, *189*, 845.
21. Miyata, T.; Tokunaga, F.; Yoneya, T.; Yoshikawa, K.; Iwanaga, S.; Niwa, M.; Takao, T.; Shimonishi, Y. *J. Biochem. (Tokyo)* **1989**, *106*, 663.
22. Nakashima, H.; Masuda, M.; Murakami, T.; Koyanagi, Y.; Matsumoto, A.; Fujii, N.; Yamamoto, N. *Antimicrob. Agents Chemother.* **1992**, *36*, 1249.
23. Tamamura, H.; Kuroda, M.; Masuda, M.; Otaka, A.; Funakoshi, S.; Nakashima, H.; Yamamoto, N.; Waki, M.; Matsumoto, A.; Lancelin, J. M., et al. *Biochim. Biophys. Acta* **1993**, *1163*, 209.
24. Tamamura, H.; Omagari, A.; Oishi, S.; Kanamoto, T.; Yamamoto, N.; Peiper, S. C.; Nakashima, H.; Otaka, A.; Fujii, N. *Bioorg. Med. Chem. Lett.* **2000**, *10*, 2633.
25. De Clercq, E. *Nat. Rev. Drug Discov.* **2003**, *2*, 581.
26. Schols, D.; Struyf, S.; Van, D. J.; Este, J. A.; Henson, G.; De Clercq, E. *J. Exp. Med.* **1997**, *186*, 1383.
27. Schols, D.; Este, J. A.; Henson, G.; De Clercq, E. *Antiviral Res.* **1997**, *35*, 147.
28. Schols, D. *Curr. Top. Med. Chem.* **2004**, *4*, 883.
29. Ichiyama, K.; Yokoyama-Kumakura, S.; Tanaka, Y.; Tanaka, R.; Hirose, K.; Bannai, K.; Edamatsu, T.; Yanaka, M.; Niitani, Y.; Miyano-Kurosaki, N., et al. *Proc. Natl. Acad. Sci. U.S.A.* **2003**, *100*, 4185.
30. Fasan, R.; Dias, R. L.; Moehle, K.; Zerbe, O.; Vrijbloed, J. W.; Obrecht, D.; Robinson, J. A. *Angew. Chem., Int. Ed. Engl.* **2004**, *43*, 2109.
31. Athanassiou, Z.; Dias, R. L.; Moehle, K.; Dobson, N.; Varani, G.; Robinson, J. A. *J. Am. Chem. Soc.* **2004**, *126*, 6906.
32. Descours, A.; Moehle, K.; Renard, A.; Robinson, J. A. *Chembiochem* **2002**, *3*, 318.
33. Favre, M.; Moehle, K.; Jiang, L.; Pfeiffer, B.; Robinson, J. A. *J. Am. Chem. Soc.* **1999**, *121*, 2679.
34. Robinson, J. A.; Shankaramma, S. C.; Jetter, P.; Kienzl, U.; Schwendener, R. A.; Vrijbloed, J. W.; Obrecht, D. *Bioorg. Med. Chem.* **2005**, *13*, 2055.
35. Shankaramma, S. C.; Athanassiou, Z.; Zerbe, O.; Moehle, K.; Mouton, C.; Bernardini, F.; Vrijbloed, J. W.; Obrecht, D.; Robinson, J. A. *Chembiochem* **2002**, *3*, 1126.
36. Shankaramma, S. C.; Moehle, K.; James, S.; Vrijbloed, J. W.; Obrecht, D.; Robinson, J. A. *Chem. Commun. (Camb.)* **2003**, 1842.
37. Müller, K.; Obrecht, D.; Knierzinger, A.; Stankovic, C.; Spiegler, C.; Bannwarth, W.; Trzeciak, A.; Englert, G.; Labhardt, A. M.; Schönholzer, P. In *Perspectives in Medicinal Chemistry*; Testa, B., Kyburz, E., Fuhrer, W., Giger, R., Eds.; Helv. Chim. Acta: Basel, 1992; p 513.
38. Obrecht, D.; Altorfer, M.; Robinson, J. A. In *Advances in Medicinal Chemistry*; Maryanoff, B. E., Reitz, A. B., Eds.; JAI Press: Stamford, Connecticut, 1999; pp 1–68.
39. Jiang, L.; Moehle, K.; Dhanapal, B.; Obrecht, D.; Robinson, J. A. *Helv. Chem. Acta* **2000**, *83*, 3097.
40. Nakamura, T.; Furunaka, H.; Miyata, T.; Tokunaga, F.; Muta, T.; Iwanaga, S.; Niwa, M.; Takao, T.; Shimonishi, Y. *J. Biol. Chem.* **1988**, *263*, 16709.
41. Tang, Y. Q.; Yuan, J.; Osapay, G.; Osapay, K.; Tran, D.; Miller, C. J.; Ouellette, A. J.; Selsted, M. E. *Science* **1999**, *286*, 498.

42. Philpott, S.; Weiser, B.; Anastos, K.; Kitchen, C. M.; Robison, E.; Meyer, W. A., III; Sacks, H. S.; Mathur-Wagh, U.; Brunner, C.; Burger, H. *J. Clin. Invest.* **2001**, *107*, 431.
43. Gupta, S. K.; Pillarisetti, K.; Thomas, R. A.; Aiyar, N. *Immunol. Lett.* **2001**, *78*, 29.
44. Kilby, J. M.; Eron, J. J. *N. Engl. J. Med.* **2003**, *348*, 2228.
45. Chantry, D. *Expert. Opin. Emerg. Drugs* **2004**, *9*, 1.
46. Tamamura, H.; Hiramatsu, K.; Kusano, S.; Terakubo, S.; Yamamoto, N.; Trent, J. O.; Wang, Z.; Peiper, S. C.; Nakashima, H.; Otaka, A., et al. *Org. Biomol. Chem.* **2003**, *1*, 3656.
47. Tamamura, H.; Hiramatsu, K.; Mizumoto, M.; Ueda, S.; Kusano, S.; Terakubo, S.; Akamatsu, M.; Yamamoto, N.; Trent, J. O.; Wang, Z., et al. *Org. Biomol. Chem.* **2003**, *1*, 3663.
48. Loetscher, M.; Geiser, T.; O'Reilly, T.; Zwahlen, R.; Baggiolini, M.; Moser, B. *J. Biol. Chem.* **1994**, *269*, 232.
49. Sune, C.; Brennan, L.; Stover, D. R.; Klimkait, T. *Clin. Microbiol. Infect.* **2004**, *10*, 119.